

Disentangling Giant Component and Finite Cluster Contributions in Sparse Matrix Spectra

Reimer Kühn

Mathematics Department, King's College London, Strand, London WC2R 2LS, UK

March 10, 2022

Abstract

We describe a method for disentangling giant component and finite cluster contributions to sparse random matrix spectra, using sparse symmetric random matrices defined on Erdős-Renyi graphs as an example and test-bed.

1 Introduction

While there has been considerable recent progress in the understanding of sparse random matrix spectra [1, 2, 3, 4, 5, 6, 7, 8], there is at least one important open problem which has not yet been properly addressed, viz. the disentangling of contributions to limiting spectra coming from the giant component and from finite clusters, respectively. This is of particular relevance when separating pure point (localized) and absolutely continuous components of random matrix spectra: contributions from finite clusters are trivially localized, yet what we are mainly interested in is to identify pure point contributions to random matrix spectra originating from the giant component, rather than the ‘trivial contaminations’ of these coming from finite clusters.

The present note is meant to address and solve this very problem. The solution is relevant also to the analysis of other forms of collective phenomena on networked systems, such as the analysis of infection dynamics or of network models of systemic risk in finance. We describe our method for the spectral problem of weighted adjacency matrices. The same method can be used to evaluate spectra of (weighted) graph Laplacians [5], sparse Markov Matrices [9, 10], or non-Hermitian sparse matrices [11].

2 Spectral Density and Resolvent

We are interested in evaluating the spectral density of sparse matrices A of the form

$$A_{ij} = c_{ij}K_{ij} , \quad (1)$$

in which $C = (c_{ij})$ is a sparse connectivity or adjacency matrix describing a finitely coordinated random graph, and $K = (K_{ij})$ a matrix of edge weights. We take both C and K to be real symmetric matrices.

The spectral density of A is obtained from the resolvent using the Edwards Jones approach [12] as

$$\rho_A(\lambda) = \frac{1}{\pi N} \lim_{\varepsilon \rightarrow 0} \text{Im} \text{Tr} (\lambda_\varepsilon \mathbb{I} - A)^{-1} = -\frac{2}{\pi N} \lim_{\varepsilon \rightarrow 0} \text{Im} \frac{\partial}{\partial \lambda} \ln Z_N , \quad (2)$$

with $\lambda_\varepsilon = \lambda - i\varepsilon$ and

$$Z_N = \int \prod_{i=1}^N \frac{du_i}{\sqrt{2\pi/i}} \exp \left\{ -\frac{i}{2} \sum_{i,j} (\lambda_\varepsilon \delta_{ij} - A_{ij}) u_i u_j \right\} . \quad (3)$$

This gives

$$\rho_A(\lambda) = \frac{1}{\pi N} \operatorname{Re} \sum_i \langle u_i^2 \rangle, \quad (4)$$

where $\langle \dots \rangle$ is an average w.r.t. the complex Gaussian measure defined by (3). Only single-site variances are needed for the evaluation. The role of ε in these equations is to ensure that integrals converge even for λ in the spectrum of A , and the limit $\varepsilon \rightarrow 0$ should be taken at the end of the calculation. However, as demonstrated elsewhere [5], there is a second role of ε , namely as a regularizer of the spectral density, and a small non-zero value of ε must be kept in the evaluation of spectral densities in order to expose pure point contributions to spectra.

This representation can be used to evaluate spectral densities for large single problem instances in terms of cavity recursions [6] as detailed below. In the thermodynamic limit these can be interpreted as stochastic recursions, giving rise to a self-consistency equation for pdfs of (inverse) variances of cavity marginals. Alternatively, thermodynamic limit results are obtained by averaging (2) over the ensemble of random matrices considered, using replica or to perform the average.

3 Cavity Analysis

As demonstrated in [6], one can use the cavity method to evaluate the marginals of the complex Gaussian defined by (3) which are needed in the evaluation of (9). We briefly repeat the reasoning here, both for completeness and in order to prepare a generalization that keeps track of the information whether a site belongs to the giant component or to one of the finite clusters of the system.

For a single-site marginal we have the representation

$$P(u_i) \propto \exp \left\{ -\frac{i}{2} \lambda_\varepsilon u_i^2 \right\} \int \prod_{j \in \partial i} du_j \exp \left\{ i \sum_{j \in \partial i} K_{ij} u_i u_j \right\} P_j^{(i)}(u_j), \quad (5)$$

with ∂i denoting the set of sites connected to i (which may or may not be empty) and $P_j^{(i)}(u_j)$ denoting the complex cavity weight of u_j . On a (locally) tree-like graph one may write down a recursion for the cavity weights,

$$P_j^{(i)}(u_j) \propto \exp \left\{ -\frac{i}{2} \lambda_\varepsilon u_j^2 \right\} \prod_{\ell \in \partial j \setminus i} \int du_\ell \exp \left\{ i K_{j\ell} u_j u_\ell \right\} P_\ell^{(j)}(u_\ell). \quad (6)$$

As demonstrated in [6], recursions of this type are self-consistently solved by complex Gaussians of the form

$$P_j^{(i)}(u_j) = \sqrt{\frac{\omega_j^{(i)}}{2\pi}} \exp \left\{ -\frac{1}{2} \omega_j^{(i)} u_j^2 \right\}, \quad (7)$$

which transforms Eq. (6) into a recursion for the $\omega_j^{(i)}$,

$$\omega_j^{(i)} = i \lambda_\varepsilon + \sum_{\ell \in \partial j \setminus i} \frac{K_{j\ell}^2}{\omega_\ell^{(j)}}. \quad (8)$$

This recursion can be solved iteratively for large single instances.

In terms of the solution, the spectral density is given by

$$\rho_A(\lambda) = \frac{1}{\pi N} \operatorname{Re} \sum_i \langle u_i^2 \rangle, \quad (9)$$

with

$$\langle u_i^2 \rangle = \frac{1}{\omega_i} \quad (10)$$

and

$$\omega_i = i\lambda_\varepsilon + \sum_{j \in \partial i} \frac{K_{ij}^2}{\omega_j^{(i)}} \quad (11)$$

Alternatively in the infinite system limit of a random system one can interpret Eq. (8) as a stochastic recursion for the collection $\{\omega_j^{(i)}\}$ of random inverse cavity variances, which in turn generates a recursion for the pdf $\pi(\omega)$ of the $\omega_j^{(i)}$.

3.1 Averaging Stochastic Recursions

Averaging single instance cavity equations to obtain equations for distributions $\pi(\omega)$ of inverse cavity variances valid for the thermodynamic limit follows standard reasoning. We have

$$\pi(\omega) = \sum_{k \geq 1} p(k) \frac{k}{c} \int \prod_{\nu=1}^{k-1} d\pi(\omega_\nu) \left\langle \delta(\omega - \Omega_{k-1}) \right\rangle_{\{K_\nu\}} \quad (12)$$

where $p(k) \frac{k}{c}$ is the probability to be connected to a site of degree k , and

$$\Omega_{k-1} = \Omega_{k-1}(\{\omega_\nu, K_\nu\}) = i\lambda_\varepsilon + \sum_{\nu=1}^{k-1} \frac{K_\nu^2}{\omega_\nu}. \quad (13)$$

We use $\langle \dots \rangle_{\{K_\nu\}}$ to denote an average over the set of (independent) edge weights appearing in the argument.

Similarly, the spectral density in the thermodynamic limit is given by

$$\rho(\lambda) = \frac{1}{\pi} \text{Re} \sum_{k \geq 0} p(k) \int \prod_{\nu=1}^k d\pi(\omega_\nu) \frac{1}{\Omega_k(\{\omega_\nu, K_\nu\})} \quad (14)$$

The problem with this approach is that it does *not* separate contributions to the limiting spectral density coming from the giant component and from finite clusters which are also represented in the graph-ensemble.

For large single instances, one could of course always identify the largest component of a system, restrict the cavity analysis of spectra to that largest component and subsequently average it over many realizations to obtain ensemble averages (albeit only finite-size approximations thereof).

In what follows we shall revisit the cavity analysis of sparse matrix spectra, and combine it with a corresponding cavity analysis of the percolation problem on the graph for which random matrix spectra are being evaluated, so as to disentangle giant component and finite cluster contributions to limiting spectral densities.

4 Cavity Approach and Ensemble Averaging Revisited

In order to disentangle contributions to the spectral density coming from finite clusters and the giant component of a graph, respectively, we need to supplement the cavity analysis of Sect. 3 by a component that allows one to keep track of the information whether a site belongs to the former or the latter.

To that end we use ideas developed for the analysis of the percolation problem of random graphs [13]. Rather than directly analysing percolation in terms of the fraction p_{gc} of vertices that belong to the giant cluster of a graph we use indicator-variables $n_i \in \{0, 1\}$ signifying whether individual sites i belong to the giant cluster of a graph ($n_i = 1$) or whether, on the contrary, they belong to one of the finite clusters of the system ($n_i = 0$).

For these we then have

$$n_i = 1 - \prod_{j \in \partial i} (1 - n_j^{(i)}) \quad (15)$$

where $n_j^{(i)}$ is a cavity indicator variable signifying whether site j does ($n_j^{(i)} = 1$) or does not ($n_j^{(i)} = 0$) belong to the giant cluster on the cavity graph, from which site i and the edges connected to it have been removed. The cavity indicator variables then satisfy the recursion

$$n_i^{(j)} = 1 - \prod_{\ell \in \partial j \setminus i} (1 - n_\ell^{(j)}) . \quad (16)$$

The structure of these equations for the indicator and the cavity indicator variables clearly mimics that for the single-site marginals Eq. (5) and the cavity marginals Eq. (6), respectively.

In the large system limit of a random graph one can interpret Eq. (16) as a stochastic recursion for the collection $\{n_i^{(j)}\}$ of cavity indicator variables that supplements the recursion Eq. (8) for the inverse cavity variances $\{\omega_i^{(j)}\}$. Combining the two then in turn generates a recursion for the *joint distribution* $\pi(\omega, n)$ of inverse cavity variances *and* cavity indicator variables, which take the form

$$\pi(\omega, n) = \sum_{k \geq 1} p(k) \frac{k}{c} \sum_{\{n_\nu\}} \int \prod_{\nu=1}^{k-1} d\pi(\omega_\nu, n_\nu) \left\langle \delta(\omega - \Omega_{k-1}) \right\rangle_{\{K_\nu\}} \times \delta_{n, 1 - \prod_{\nu=1}^{k-1} (1 - n_\nu)} \quad (17)$$

From the solution of this equation one obtains the limiting spectral density as a sum of two contributions, one of these (ρ_{gc}) coming from the giant cluster, the other (ρ_{fc}) from the collection of finite clusters,

$$\rho(\lambda) = \rho_{\text{gc}}(\lambda) + \rho_{\text{fc}}(\lambda) , \quad (18)$$

with

$$\rho_{\text{gc}}(\lambda) = \frac{1}{\pi} \text{Re} \sum_{k \geq 0} p(k) \sum_{\{n_\nu\}} \int \prod_{\nu=1}^k d\pi(\omega_\nu, n_\nu) \frac{1}{\Omega_k(\{\omega_\nu, K_\nu\})} \times \delta_{1, 1 - \prod_{\nu=1}^k (1 - n_\nu)} , \quad (19)$$

$$\rho_{\text{fc}}(\lambda) = \frac{1}{\pi} \text{Re} \sum_{k \geq 0} p(k) \sum_{\{n_\nu\}} \int \prod_{\nu=1}^k d\pi(\omega_\nu, n_\nu) \frac{1}{\Omega_k(\{\omega_\nu, K_\nu\})} \times \delta_{0, 1 - \prod_{\nu=1}^k (1 - n_\nu)} , \quad (20)$$

with $\Omega_k(\{\omega_\nu, K_\nu\})$ as defined above.

Eq. (17) is efficiently solved by a population dynamics algorithm [14], and the giant component and finite cluster contributions to the spectral density are evaluated by sampling from the equilibrium distribution of the population dynamics.

Both $\pi(\omega, 1)$ and $\pi(\omega, 0)$ have support in the complex half-plane $\text{Re } \omega \geq 0$. As argued in [5], a pure point contribution is signified by a singular component of $\pi(\omega, n)$ with support on the imaginary axis $\omega \in i\mathbb{R}$.

5 Results and Discussion

In what follows, we briefly illustrate the workings of our method by providing sample spectra of sparse matrices of the type (1). Here we present results for matrices defined on a sparse Erdős-Renyi graph of mean connectivity $c = 2$. It goes without saying that other matrix and graph ensembles can be analysed in the same way, in the sense that the method of disentangling giant and finite cluster distributions described here is not restricted to Erdős-Renyi graphs but works for any system in the configuration model class, as well as for spectra of weighted graph Laplacians [5] or of sparse random stochastic matrices [9, 10].

In Fig. 1, we present the spectrum of a matrix with Gaussian random edge weights of standard deviation $\sigma = 1/\sqrt{c}$ on the edges of the Erdős-Renyi graph, separately exhibiting the contributions coming from the giant cluster and from the collection of finite clusters. The former occupies a fraction $p_{\text{gc}} \simeq 0.796812$ of the entire system. We also compare our results with simulations, associating the giant cluster with the largest finite cluster of each realization of the system, and all other components with the collection of finite clusters, finding excellent agreement with theoretical results. Note that the finite cluster results displayed in the right panel of

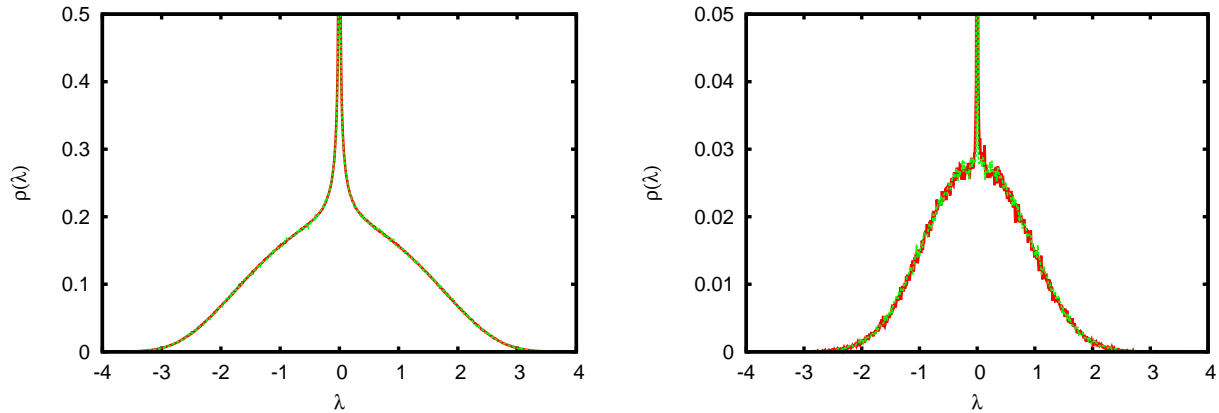


Figure 1: (Colour online) Spectral density of a random matrix defined on an Erdős-Rényi random graph of mean connectivity $c = 2$, with link weights normally distributed with standard deviation $\sigma = 1/\sqrt{c}$. Left panel: giant-cluster contribution. Right panel: finite-cluster contribution. In both panels, full red lines represent results for the limiting spectral density obtained via population dynamics, while green dashed lines are simulation results using graphs of $N = 500$ vertices, averaged over 5000 random instances. Note the different vertical scale in the right panel.

Fig. 1 are slightly noisier than those pertaining to the giant cluster, as a smaller fraction of updates in the population dynamics corresponds to finite cluster contributions.

In Fig. 2 we show results for the spectrum of the adjacency matrix on the giant cluster of an Erdős-Rényi graph, with edge weight set at $1/\sqrt{c}$. As shown in [15], all eigenvalues which are eigenvalues of finite trees will also appear as eigenvalues of the adjacency matrix of the giant component of the system, and correspond to localized states. The left panel of Fig. 2 exhibits a few of these, namely the ones with the largest weights appearing in the giant component spectrum; the weight of the remaining atoms is too small, entailing that these are ‘drowned’ in the continuum at the resolution (and regularization) chosen in the figure. In the right panel the continuum contribution is subtracted, so that it exhibits just the contribution of localized states to the spectrum of the giant component of the system, regularized at $\varepsilon = 10^{-3}$. Note that one effect of regularization is to broaden each δ -peak into a Lorentzian of width ε , which is clearly visible for the peaks with the largest weight in the spectrum. The system also exhibits Anderson localization, entailing that *all* states with $|\lambda| > \lambda_c \simeq 2.50$ are localized; this corresponds to the two bands of states at $|\lambda| > \lambda_c$ in the right panel of Fig. 2. As expected we find *all* states on finite clusters to be localized.

A numerical integration (using a trapeze-rule) of the total density of states on the giant cluster gives

$$\int d\lambda \rho_{\text{gc}}(\lambda) \simeq 0.7969 \quad (21)$$

which agrees very well with the expected result $p_{\text{gc}} \simeq 0.796812$, i.e. the fraction of vertices of the system in the giant cluster. Doing the integration for the (absolutely)-continuous component of the giant-cluster spectrum gives

$$\int d\lambda \rho_{\text{gc}}^{(\text{ac})}(\lambda) \simeq 0.7153 \quad (22)$$

entailing that a fraction

$$f_{\text{gc}}^{(\text{loc})} \simeq \frac{0.7969 - 0.7153}{0.7969} \simeq 0.1020, \quad (23)$$

i.e. approximately 10% of all states on the giant cluster are localized.

To summarize, by combining approaches to percolation on random graphs and to the evaluation of sparse matrix spectra we have presented a method that allows to separately evaluate contributions to sparse matrix spectra coming from the giant cluster and from finite clusters, respectively. Our results are confirmed to a high precision by numerical simulations, even at moderate system size.

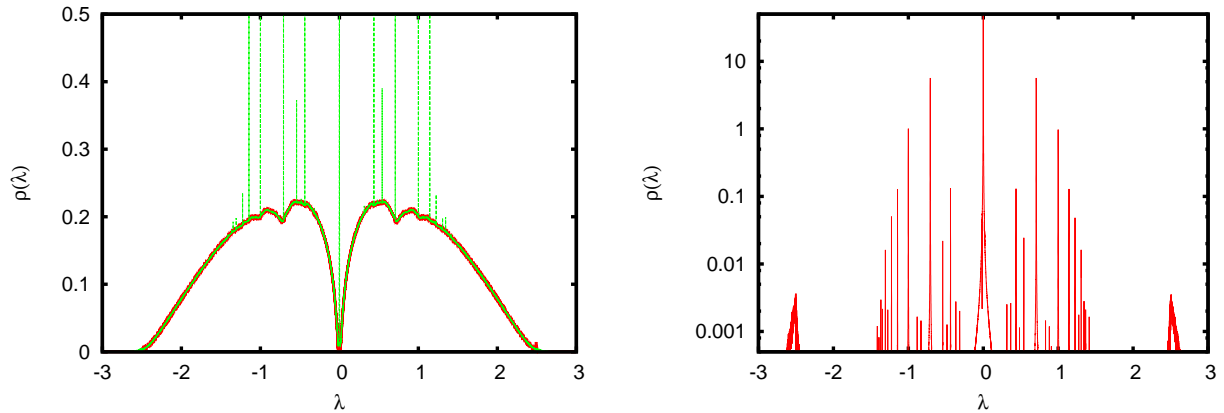


Figure 2: (Colour online) Spectral density of the adjacency matrix of the giant cluster of an Erdős-Renyi random graph of mean connectivity $c = 2$, with link weights chosen as $1/\sqrt{c}$. Left panel: continuous density of states (thick full red line) and total density of states including atoms (green dashed line). Right panel: spectrum of *localized* states on the giant cluster regularized at $\varepsilon = 10^{-3}$. The central part of the panel exhibits atoms in the bulk of the spectrum, whereas the two bands in the vicinity of ± 2.5 correspond to fully localized bands of states, separated by mobility edges from the bulk of the spectrum. The normalization is chosen such that the total DOS integrates to the fraction of sites contained in the percolating cluster (see Eq. (21)).

By further disentangling the absolutely continuous and pure point contribution to limiting spectra, we are able to give a precise estimate of the fraction of states *on the giant cluster* that are localized. We are not aware of a previous such estimate, although a method to estimate the weight of the peak at $\lambda = 0$ was recently devised by Bordenave et al. [16].

We expect our method to be useful for the analysis of other phenomena described in terms of networked systems, including e.g. the spread of diseases or computer viruses, the behaviour of random walks or the performance of search algorithms on networks.

A interesting field of research, where our results can provide a crucial ingredient of the analysis is the investigation of localization phenomena, where it is important to avoid contamination of results from finite cluster contributions.

Acknowledgements Illuminating discussions with Justin Salez and with Peter Sollich are gratefully acknowledged.

References

- [1] G. J. Rodgers and A. J. Bray. Density of States of a Sparse Random Matrix. *Phys. Rev. B*, 37:3557–3562, 1988.
- [2] G. Biroli and R. Monasson. A Single Defect Approximation for Localized States on Random Lattices. *J. Phys. A*, 32:L255–L261, 1999.
- [3] G. Semerjian and L. F. Cugliandolo. Sparse Random Matrices: The Eigenvalue Spectrum Revisited. *J. Phys. A*, 35:4837–4851, 2002.
- [4] S. N. Dorogovtsev, A. V. Goltsev, J. F. F. Mendes, and A. N. Samukhin. Spectra of Complex Networks. *Phys. Rev. E*, 68:046109, 2003.
- [5] R. Kühn. Spectra of Sparse Random Matrices. *J. Phys. A*, 41:295002 (21pp), 2008.

- [6] T. Rogers, I. Pérez Castillo, R. Kühn, and K. Takeda. Cavity Approach to the Spectral Density of Sparse Symmetric Random Matrices. *Phys. Rev. E*, 78:031116, 2008.
- [7] L. Erdős, A. Knowles, H. T. Yau, and J. Yin. Spectral Statistics of Erdős-Renyi Graphs I: Local Semicircle Law. *Ann. Prob.*, 41:2279–2375, 2013.
- [8] C. Bordenave, P. Caputo, and D. Chafaï. Spectrum of Markov Generators on Sparse Random Graphs. *Comm. in Pure and Appl. Math.*, 67:621–669, 2014.
- [9] R. Kühn. Spectra of Random Stochastic Matrices and Relaxation in Complex Systems. *Europhys. Lett.*, 109:60003, 2015.
- [10] R. Kühn. Random Matrix Spectra and Relaxation in Complex Networks, 2014.
- [11] T. Rogers and I. Pérez Castillo. Cavity Approach to the Spectral Density of Non-Hermitian Sparse Matrices. *Phys. Rev. E*, 79:012101, 2009.
- [12] S. F. Edwards and R. C. Jones. The Eigenvalue Spectrum of a Large Symmetric Random Matrix. *J. Phys. A*, 9:1595–1603, 1976.
- [13] M. E J. Newman, S. H. Strogatz, and D. J. Watts. Random Graphs with Arbitrary Degree Distributions and their Applications. *Phys. Rev. E*, 64:026118, 2001.
- [14] M. Mézard and G. Parisi. The Bethe Lattice Spin Glass Revisited. *Eur. Phys. J. B*, 20:217–233, 2001.
- [15] M. Bauer and D. Golinelli. Random Incidence Matrices: Moments of the Spectral Density. *J. Stat. Phys.*, 103:301–337., 2001.
- [16] C. Bordenave, M. Lelarge, and J. Salez. The Rank of Diluted Random Graphs. *Ann. Probab.*, 39:1097–1121, 2011.